UNIVERSITY OF CALIFORNIA

Los Angeles

Origin and Properties of the Electrocardiogram T-Wave

A thesis submitted in partial satisfaction

of the requirements for the degree Master of Science

in Physiological Science

by

Anna Alexandra Frid

2012

ABSTRACT OF THE THESIS

Origin and Properties of the Electrocardiogram T-Wave

by

Anna Alexandra Frid

Master of Science in Integrative Biology and Physiology

University of California, Los Angeles, 2012

Professor Alan Garfinkel, Chair

The ventricle exhibits gradients in repolarization time in both transmural and apicobasal directions. These gradients, caused by the varying strengths of cellular ionic currents in the different regions, affect the morphology of the electrocardiographic T wave. Abnormal gradients, observed clinically by alterations in the ECG, can increase susceptibility to arrhythmias, and therefore the characteristics of both gradients as well as their roles in manifesting the T wave must be understood. The UCLA rabbit ventricular action potential model is based on experimental data from rabbit ventricular myocytes along with reported ion channel properties. To recreate the repolarization gradients in the ventricle, alterations were made to the conduction of repolarizing currents, I_{Kr} and $I_{to,f}$ in the single cell model to simulate the different APDs observed in-situ. The resulting cells were then incorporated into a 3D ventricle model. Simulations were performed with varying presence and direction of repolarization gradients, and an in-silico ECG was calculated. It was found that transmurally, APD epi must be shorter than APD endo and apicobasally, APD base must be shorter than APD apex to give a correct ECG.

The thesis is of Anna Alexandra Frid is approved.

Mark Frye

Victor Edgerton

Alan Garfinkel, Committee Chair

University of California, Los Angeles

2012

Dedication

I'd like to dedicate this thesis to the people who have encouraged me throughout my time at UCLA. First my advisor, Professor Dr. Alan Garfinkel, who mentored, inspired, and enlightened me as I pursued my research. His guidance was invaluable and I am grateful for his faith in me. Second the amazing team that I have been privileged to be a part of at UCLA, especially Peter Borgstrom and Shankarjee Krishnamoorthi who were essential in this project. Finally I'd like to also dedicate this to my parents, Alex and Marina Frid, along with my amazing family whose support of me has never wavered.

Table of Contents

Introduction

Cardiomyopathy increases susceptibility for severe cardiac arrhythmia and thus is an important concern for patients and clinicians. The left ventricle is responsible for delivering oxygenated blood to all other organ systems of the body. Years of damage, genetic disorders, or physiological events can lead to heart disease. Proper conduction of the electrical signal and its propagation within the myocardium is imperative for activation and depolarization of the cardiomyocytes. Repolarization is the summation of the intrinsic characteristics of the individual cells ensuing from ion channel properties, channel density and distribution, autonomic modulation, and cell-cell coupling effects. The differences observed in ventricular cells mediate the distinct repolarization times of varying regions in the myocardium which affects the electrocardiographic T wave. Direction and magnitude of repolarization in both the transmural and apico-basal direction influences T wave morphology. To elucidate the mechanism of repolarization that results in the physiological T wave, the UCLA rabbit cell model is incorporated into a 3D model of the ventricle with a purkinje network. The UCLA cell model of the rabbit action potential is based on experimental data from rabbit ventricular myocytes along with reported ion channel properties. To reproduce the repolarization gradients observed in the myocardium, conduction of repolarizing currents I_{Kr} and $I_{to,f}$ is modified in the single cell model to simulate the varying action potential durations (APDs) observed in-situ in the different regions of the heart. The resulting cells are incorporated into the 3D ventricle model in the following manner: the ventricle was first divided transmurally (Epicardial/ Endocardial/ Midmyocardial) and then apicobasally (Apex/ Center/ Base) to create 9 regions with distinct APD properties. Several experiments were performed in which the magnitude and

direction of repolarization gradients was varied, and a virtual ECG was recorded for each scenario allowing for a comparison. The six simulations represented six different cell APD compositions in the ventricle. First a homogenous APD distribution is simulated, second a transmural-only APD gradient is applied (APD epicardium < APD endocardium < APD midmyocardium), for the third and fourth simulation direction of the apico-basal gradient is tested without the transmural gradient (APD apex < APD base & APD base < APD apex). In the last two simulations the transmural gradient is combined individually with the two variations in the apico-basal gradient. The resulting calculated ECG gave understanding into the function and contribution of the gradients in the formation of the T wave. Both the transmural and the apico-basal gradient are essential in reproducing the physiological T wave when compared to an experimental rabbit ECG. Transmurally, APD epicardium must be shorter than APD endocardium, and apicobasally, APD base must be shorter than APD apex. All other variations in the direction and presence of these repolarizing gradients did not produce a physiologically correct T wave. Simulation of the ventricle with proper repolarizing gradients can be useful in studying local dispersion of repolarization and T wave alternans, both of which have been linked to increased susceptibility for cardiac arrhythmia. Thus, appreciating the role of transmural and apico-basal gradients and their foundation at the cellular level can contribute to further insight into the shifts observed in the ECG in various pathological conditions.

Cardiovascular Pathway of Electrical Conduction:

The electrical pathway of the heart begins with the sinoatrial node (SA node) located in the upper region of the right atrium (RA), at the crista terminalis junction between the RA and the superior vena cava. The SA node is made up of none contractile tissue whose pace maker cells are able to generate action potentials (APs) without extrinsic regulation of chemical signals. At the resting potential of -60mV[1] diastolic depolarization is initiated by the "funny" current (I_f). The I_f current is activated in hyperpolarization causing an influx of a mixture of sodium and potassium ions, both of which the ionic channel is permeable to.[2] As the voltage rises the transient T-type calcium channel ($I_{Ca,T)}$ is activated allowing for calcium ions to influx causing further increase. The $I_{Ca,T}$ inactivates fast but the depolarization is sustained by the long lasting L-type calcium channel ($I_{Ca,L}$). The upstroke of the pacemaker action potential is largely due to the calcium influx as the voltage reaches its peak at 10mV. As the $I_{Ca,L}$ ion channel begins to inactivate, repolarization initiates, led by the outward potassium current (I_K). The SA node has a heterogeneous cell mixture, showing variation in two types of nodal cells.[1,3] In the center of the SA node are "P" cells that make up a small percentage of the overall, but lead the pacemaking function. In the periphery and at the borders between nodal and atrial cells there are perinodal or transitional "T" cells which are responsible for the transmission of the signal to the atrial cardiomyocytes. Their properties vary in cell structure and the dominant ionic current that makes up the AP upstroke. The $I_{Ca,L}$ is primarily responsible for depolarization in the "P" cells and the voltage gated sodium ion channel ($I_{Na)}$ is the principal current in the "T" cells. At a conduction velocity of .5m/s the wave of depolarization propagates to the right and left atrial muscle. The

electrical potential spreads from cell to cell as it reaches atrioventricular node (AV node) located in inferoposterior region of interatrial septum.[4] The AV nodal region is split into three cell types. The atrionodal (AN), nodal (N), and nodal-his (NH) cells vary in their electrophysiology.[6] The AP upstroke of atrionodal and nodal-his cells' is mediated by the inward sodium current (I_{Na}), unlike SA nodal "P" cells that primarily have calcium ions influx during the first phase of depolarization.

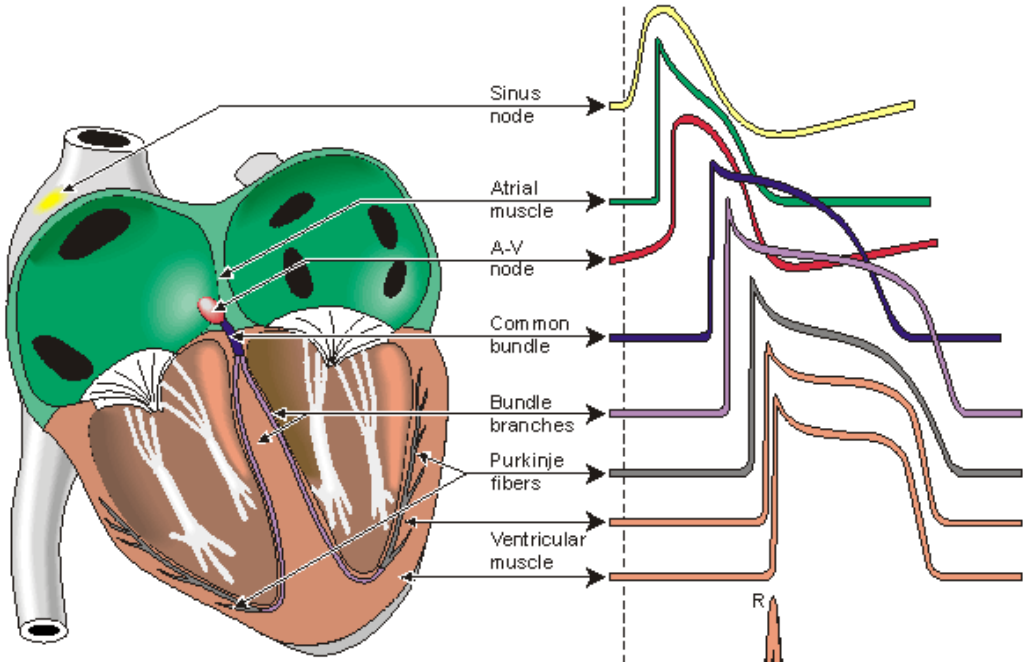

Fig 1: *Illustrates the pathway of electrical conduction of the heart with respective variation in action potentials of the SA, AV, atrial, ventricular, and his-purkinje cells. Modified from Malvivuo and Plonsey et al., R Oxford University Press. 1995, 121-124.*[29]

The AV node has the slowest conduction velocity (CV) averaging .05m/s. The low CV functions as a protective measure for possible SA node dysfunction. If multiple signals are sent from the SA node to the AV node, the difference in conduction between the two tissues enables precise propagation and protects the ventricles from irregular activation. From the AV node the electrical signal travels down the septum and into the ventricular myocardium via the Bundle of His which

diverges into right and left bundle branches. The left bundle branch splits into anterior and posterior fascicle. Both the right and left bundle branches are none contractile tissue with conduction velocity of 2m/s. The branches travel down to the apex of the heart and disperse into purkinje fibers. Purkinje cells propagate the electrical signal quickly with a high CV into the ventricular cardiomyocytes. The depolarization wave travels from cell to cell via gap junctions. Gap junctions are transmembrane proteins that enable diffusion of nutrients, ions, and small chemical signals between adjacent cells. A gap junction is formed when two connexons (hemichannels)[5,7] interact. Each connexon is assembled from 6 smaller subunits known as connexins. Connexin protein expression varies in different cardiovascular tissue.[10] The principal gap junction gene variants found in the SA node, AV node, and the conduction system are Cx40, Cx43, and Cx45. In the atrial cardiomyocytes Cx40 and Cx43 are in high concentrations. Gene variant Cx45 has also been found in the atria, but to a lesser extent. In the ventricles, cardiomyocytes contain Cx43 as the primary gap junction. However gene variants Cx45 and Cx40 have also been identified in ventricular tissue, with Cx45 being more profuse. Furthermore the association of connexons in a functional gap junction can either be homotypic, in that two of the same variants come together, or heterotypic, where different gene products constitute the hemichannels.[8,9] Each of the 6 connexins can either be uniform or vary thus affecting the function of the final protein. Gap junction protein composition differences act as a barrier, resulting in unidirectional[10] flow between adjacent tissue of the atria and ventricles. Propagation and conduction of the electrical signal is guided by the distribution of Gap junctions. Different variants can thus affect conduction velocity and therefore tissue susceptibility for episodes of arrhythmia. The concept of source-sink is characterized by the dispersion and diversity of gap

junctions. The “sink”, made up of adjacent cells connected via gap junctions, limits the time of depolarization in a cell. Occurrence of arrhythmia can be curtailed by ionic diffusion. Gap junction gene mutations and protein malfunctions can make the tissue a substrate for conduction blocks or irregular signal propagation by creating regions of uncoupled tissue.[15] Contraction of atrial and ventricular muscles is dependent upon the transmission of depolarizing signal from the nodal cells to the contractile cardiomyocytes, whose activity and resulting action potential are mediated by multiple ion channels.

Cellular Action Potential

The atria and ventricles have longer APs with prolonged plateau phases when compared to the pacemaker tissue. Split into 4 individual segments; depolarization begins at phase 0, followed by phase 1 or initial transient repolarization, the plateau in phase 2, full repolarization in phase 3, and returning to the resting potential in phase 4. (Fig. 2) Mediated by many ionic currents of voltage gated ion channels cellular activation propagates resulting in contraction of the myocardium.[11] The resting potential in the ventricular cardiomyocyte is -90mV, which is proximal to the reversal potential of potassium (E_K). The AP reaches its maximal voltage at +20mV, nearing the reversal potential of sodium (E_{Na} = +55mV). As ions travel from adjacent cells they interact with voltage gated ion channels imbedded in the cellular membrane. The upstroke in phase 0 is mediated by fast sodium conduction. The I_{Na} (SCN5A gene) channel is triggered to open at roughly -60 mV initiating the influx of sodium.[12] As the depolarized potential is reached, the calcium independent transient outward potassium current, I_{to} (KCND3 gene), is activated. This initiates early repolarization of the cardiomyocyte. I_{to} is split into two phenotypically different alpha subunits of the ion channel, a fast recovering $I_{to,f}$ (Kv 4.3) and a

slow recovering $I_{to,s}$ (Kv 1.4).[14] I_{to} gene expression varies with each animal species observed. The fast transient outward potassium current dominates in adult ferrets, dogs, and humans but less $I_{to,f}$ is observed in the rabbit ventricle, and it isn't identified in the guinea pig.[13] The plateau of phase 2 in the action potential of the ventricles and atria is maintained by the influx of calcium ions via the L-type calcium channel ($I_{Ca,L}$). When calcium diffuses into the cell the calcium-induced calcium release (CICR) mechanism will be initiated.[15]

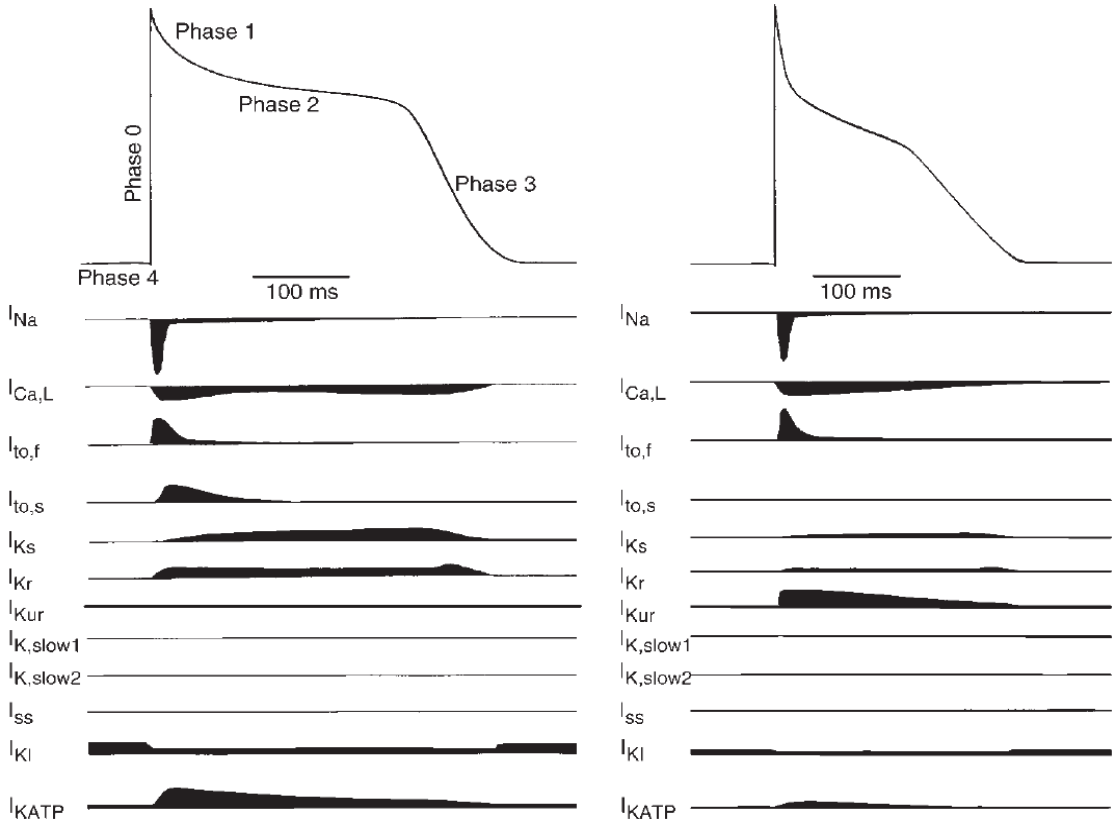

Fig 2: *Ventricular (left) and atrial (right) action potentials. Participating ionic currents are listed. Downward shading indicates inward current and upward shading indicates outward flow. Reproduced from Nerbonne & Kass et al., 2005. Physiol Rev 85, 1205-1253.*[21]

Found within the cardiomyocyte is a modified endoplasmic reticulum, which is identified as the sarcoplasmic reticulum (SR). SR functions as a modified storage unit for calcium. Influxing

positive ions interact with ryanodine receptors found on the T-tubules or invaginated regions of the modified myocyte membrane known as the sarcolemma. Activated ryanodine receptors in turn activate dehydropiridine receptors (DHPR) on the SR which causes the opening and release of stored calcium. In turn the calcium will bind proteins that inhibit the contractile myofilaments in the cell, thereby enabling contraction via excitation-contraction coupling.[15] As the intracellular calcium concentration reaches a maximum, activation of different cellular ion channels will result in a decline. The sodium calcium exchanger ($I_{Na/Ca}$) extrudes 1 calcium ion for every 3 sodium ions that enter the cell. Furthermore the SR Ca ATPase (SERCA)[16] pump participates by using adenosine triphosphate (ATP) to power calcium return into the sarcoplasmic reticulum for storage. Simultaneously in phase 3 of the AP, activated voltage gated potassium channels assist in repolarization of the cell. The delayed rectifier potassium current, I_K (Kv), can be split into two primary components in the ventricles, the rapid activating and the slow activating current. The rapidly activating potassium current, I_{Kr} (Kv 11.1/hERG), leads in phase 3 repolarization. Its distribution and concentration in the heart varies between species and influences the time of repolarization in the cardiomyocyte.[21] The slow activating current, I_{Ks} (Kv 7.1, KvLQT1), has a distinct time course from its fast counterpart and influences the action potential. Dispersion and conduction of these currents affects the direction of repolarization in the ventricle. Besides the voltage gated potassium Kv channels, there are three distinct inward rectifier currents (I_{K1}, I_{KATP}, and $I_{K(ACh}$). In the ventricles two channels, I_{K1} and I_{KATP}, are in high density and participate in shaping the AP.[17] I_{K1} activates at rest and closes at depolarization. It has slowed conduction from positive voltages to -40mV. Below E_K, the inward potassium current conduction is larger than the outward force above -90mV.[18] At positive potentials I_{K1} is considered to be blocked by a

handful of molecules such as Mg^{2+} and polyamines. The I_{K1} inward rectifier current is also considered to assist in repolarization as the AP reaches the resting potential. Research has shown that when the I_{K1} channel is blocked the resting potential becomes depolarized. [18] Furthermore when if I_{K1} activity is impeded the AP is prolonged affecting the steepness of the slope during repolarization. Under normal physiological conditions I_{KATP} does not alter the overall AP, but during myocardial stress it takes on an important role in the cellular reaction to ischemic events.[19] ATP blocks the sensitive channel, but during ischemia, with a given lack of oxygen and ATP production, the I_{KATP} channel is in an open state. This will cause a shortening of the AP duration, specifically affecting the speed of repolarization via the extrusion of potassium ions.[20] The maintenance of the resting potential is also supported by the sodium potassium ATPase, which creates a negative net voltage in the cell by pumping out 3 sodium for every 2 potassium that enter. The ions are traveling against their concentration gradients with the use of ATP. The assembly, distribution, and kinetic properties of these ion channels comprise the normal action potential. The resulting electrical signal that is sent throughout to the contractile tissue is further modified by the autonomic nervous system.

Autonomic Innervation of the Heart

Due to the pacemaker activity of the sinoatrial node and its conduction pathway the heart can maintain basic electrical activity without the neural influence. However, the autonomic nervous system (ANS) is imperative in adjusting the pace and contractility of the heart during basal activity and varying physiological conditions.[23] The ANS can be split into the sympathetic and parasympathetic nervous systems (Fig. 3), which work in conjunction with each other to modify heart rate and blood pressure. Sympathetic nerves extend from the medulla into the paravertebral

ganglia. When activated these neurons synapse on different regions of the heart.[29] The sympathetic nervous system (SNS) interacts with the nodal cells, the his-purkinje fibers, and the contractile cells of the atria and ventricles. When acting on the cardiomyocytes, the SNS is known to increase heart rate, conduction velocity, and contractility.[22] Alpha and beta adrenergic receptors are embedded in the target tissue. Adrenergic receptors interact with the SNS neurotransmitter norepinephrine (NE), as well as the endogenous circulating catecholamine, epinephrine (EPI). The dominant adrenergic receptors in the ventricles are the beta-1 and beta-2 receptors.[24]

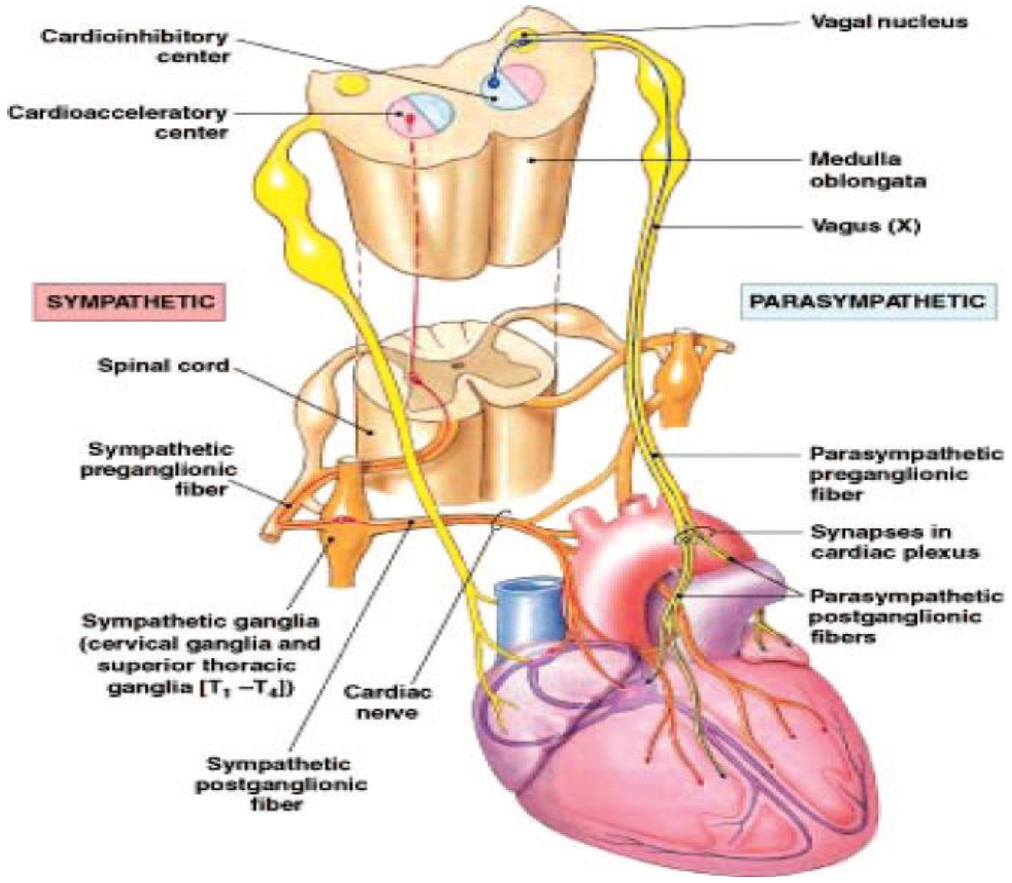

Fig 3: *The pathways of the Autonomic Nervous System. The sympathetic fibers and the vagal parasympathetic fibers innervating different regions of the atria and ventricles are highlighted. Reproduced from Olshansky et al., 2008. Circulation 118, 863-871.*[28]

Binding of the adrenergic receptors by their agonists causes an increase in cellular contraction via the G-protein mediated signal conduction pathway. The G-protein activation results in an upsurge in production of the second messenger, cAMP, which in turn will cause the activation of protein kinase A (PKA). PKA will then phosphorylate a multitude of key enzymes ensuing in a cascade of effects that will increase intracellular calcium release as well as the cell's ability to contract and relax at a faster rate. Beta-1 adrenergic receptor is found in higher concentration than beta-2, but research has shown that beta-2 adrenergic receptor's role is primary in heart failure. [25] Long term stress and SNS overstimulation results in the downregulation of production and activity of the beta-1 receptors. Another type of adrenoceptor found in the cardiac cells is the alpha-1. When bound by its neurotransmitters and other agonists the receptor acts by increasing inotropy in the cardiomyocytes via calcium release and increase in calcium sensitivity of the contractile proteins.[26,27] The SNS is countered by the parasympathetic nervous system (PNS) whose nerves release acetylcholine (ACh) as the primary neurotransmitter.[28] The vagal nerve extends to the target tissue which have muscarinic acetylcholine receptors (mAChR) embedded in their cellular membranes.[26] Activation of the mAChR results in a G protein mediated signal transduction cascade that causes a decrease in heart rate and contractility in the ventricles. The predominant muscarinic receptor in the heart is the M_2 which is located in the atria and ventricles. Both muscarinic and adrenoceptors are found in the prejunctional neurons as well allowing for communication between the two nervous systems. The parasympathetic vagal "tone" is found to dominate at rest over the sympathetic. This complex realtionship of the two systems does not only influence the basal heart rate, but can be seen as a therapeutic target in heart disease.[30]

Electrocardiogram:

Clinicians utilize electrocardiography to view the electrical activity of the heart and deduce possible pathology when an abnormal electrocardiogram (ECG) arises. The goal of this study is to apply the knowledge of the cellular properties that result in a 12-lead ECG in order to simulate a physiologically representative virtual electrocardiogram. Depolarization is spread from cell to cell via gap junctions in the heart which can be paralled to an electrical conductor. The voltage difference between regions of the heart is measured and the rate of change in electrical potential across the myocardium can be quanitfied. Composite waveforms stemming from body surface electrodes are presented in the graphic. The twelve lead ECG consists of 3 standard bipolar leads, 3 augmented and 3 precordial unipolar leads. The 3 standard leads are placed at the left arm (LA), right arm (RA) and left leg (LL).[31] Lead I represents the difference measured between RA and LA electrodes. Lead II is the difference between LL and RA electrodes and lead III is the difference between LL and LA electrodes. The methodology for the first three leads is based on the Einthoven triangle.[33] Using lead I-III, the augmented vector left (aVL), the augmented vector right (aVR), and augmented vector foot (aVF) is calculated. The magnitude of each vector is altered by the bipolar lead placement on the body. Based on the Wilson's Central Terminal theory,[34,35] each of the augmented leads acts as a unipolar positive electrode, with a corresponding composite negative electrode made up of the difference in potential in the three standard leads. The six leads are able to measure the potential changes in the frontal plane of the body, represented on an hexaxial reference system (Fig. 4). The last six leads in the 12 lead ECG are composed of electrodes placed directly on the chest to view the activity in the transverse plane of the body. Lead V1 through V6 are know as precordial leads and are unipolar positive

electrodes.[31] The resulting waveform visualized in an ECG at each lead is dependent on the magnitude and direction of the mean electrical axis. The wave of electrical activity diffuses in all directions and therefore the mean electrical axis is the sum of all the mean electrical vectors in the heart. When a wave of depolarization moves towards an electrode an upward deflection is recorded in the ECG. A downward deflection is noted when the depolarization wave is moving away from an electrode. Repolarization of the heart is represented by an upward waveform when the wave travels away from the electrode. A downward deflection is recorded if the repolarization wave is moving towards the respective electrode.

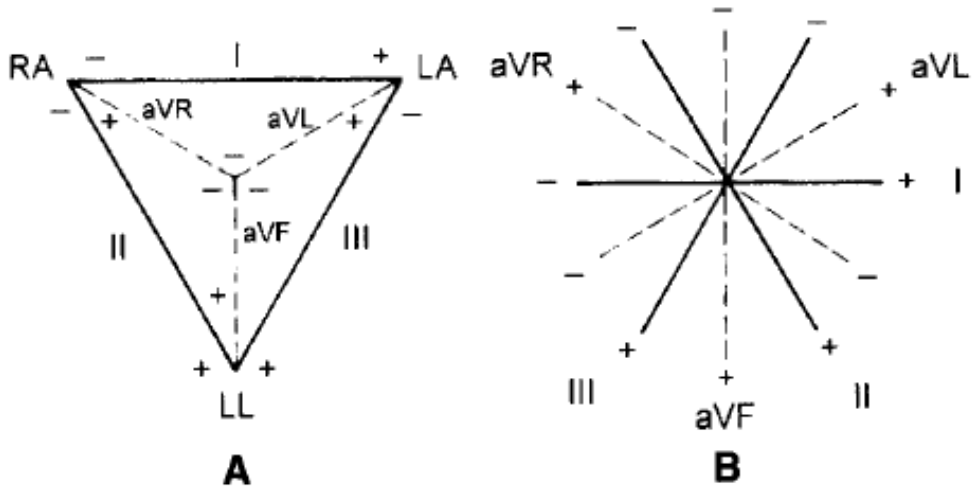

Fig 4: ***(A)*** *Frontal plane leads (I-III) with their corresponding augmented leads (aVL, aVR, aVF). Visualized within Einthoven's triangle.* ***(B)*** *The hexaxial reference system showing all 6 leads. Bipolar leads are represented by the solid lines and augmented leads are represented as dashed lines. Reproduced from Dupre et al., 2005 Handbook of Cardiac Anatomy, Physiology, and Devices 191-201.*[31]

Changes in voltage and polarity are categorized by five distinct waveforms in the representative electrocardiogram of each recording lead, denoted as P,Q,R,S,T (Fig. 5). The amplitude of the individual wave is dependent on the amount of tissue acting instantaneously in creating an

electrical gradient. The conduction pathway begins with the depolarization of the atria with a mean vector angle that is read as an upward P wave. Measurement of atrial repolarization is largely overshadowed by the ventricular depolarization. The AV node propagates the signal into the ventricular septum resulting in a small Q deflection followed by a large R and S wave denoting depolariation of the ventricular myocardium.[36] The QRS complex represents the sequential stages of depolarization in the heart. As the activation wave travels into the septum, cardiac tissue in the left ventricle is depolarized first. Then the electrical wavefront enters the right side of the ventricle. It propagates into the inner apical regions of the heart. As depolarization spreads it moves from the endocardial to the epicardial tissue in the myocardium as the signal travels up to the posterobasal cardiomyocytes.[32] Repolarization of the ventricles is represented in the ECG by the T-wave. The time of repolarization varies from cell to cell and is imperative in understanding ventricular function. An abnormal ECG waveform is a sign of possible conduction issues or cardiomyopathy in the heart. Duration, height, and shape of each wave has a standard range, but when a distortion is observed a possible arrhythmia can be identified and treated. Variation in the P wave morphology with either disturbed or chaotic waveforms are representative of atrial arrhtyhmias such as atrial flutter and atrial fibrillation. The distance between the beginning of the P wave and the start of QRS complex is known as the PR interval. It encompasses the time between atrial depolarization and the propagation of the electrical signal into the AV node and the ventricles. Increase in the duration of the PR interval can signify conduction block, in which the signal is either being delayed at the AV node or is not transmitting properly. The QRS complex properties are an overview of the initiation and the bulk of ventricular depolarization. Reasearch has highlighted a possible correlation between QRS

interval widening to an increased risk of death in cardiomyopathy.[38,39] Alterations in the waveform of the QRS complex can result from either ventricular damage after an incident of myocardial infarct (MI) or from conduction block due to heart failure and cellular modification caused by physical stress and hypertrophy. In particular fragmented QRS (fQRS)[40] is observed in the ECG with distinct characteristics ensuing from scaring of the myocardium. Visually fQRS has the presense of an R' wave which is a deflection in the nadir of the S wave resulting in a second refraction. The variation in RSR' waveform is the product of complications in the ventricular depolarization pathway due to prior MI occurrence.

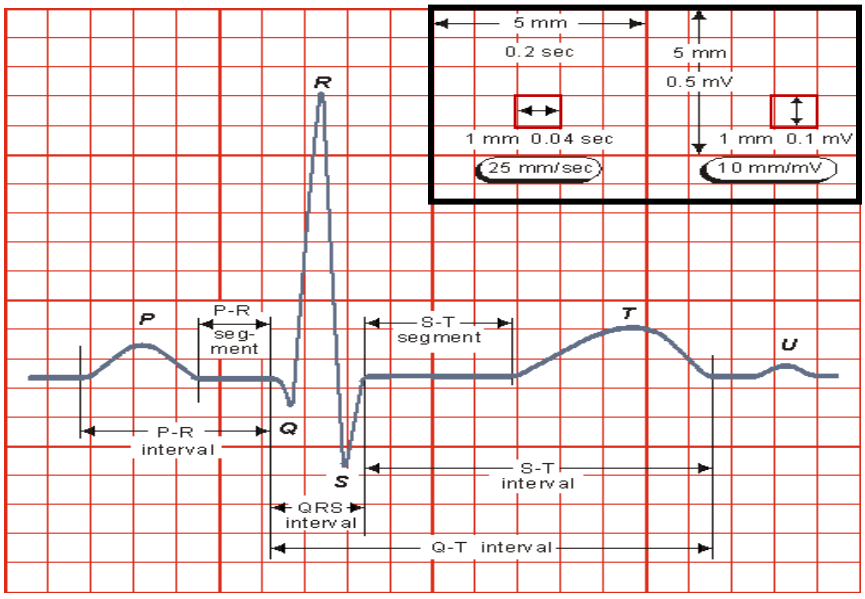

Fig 5: *ECG Overview: Single cardiac cycle electrocardiogram. Dimensions of the ECG paper (upper right corner) focusing on the single square-- with 1mm in width as 0.04 sec and 1mm in height is 0.1mV. PQRSTU waves denoted and respective PR interval, PR segment, QRS complex, ST segment, ST interval, and QT interval identified. Modified from Malvivuo and Plonsey et al., R Oxford University Press. 1995, 121-124.*[29]

Between the end of the QRS complex and the beginning of the T wave, is the ST segment. At the cellular level the ST segment duration spans the first and second phase of the AP. During this period of time the initial I_{to} activated repolarization is countered by the calcium influx observed

in the plateau. ST segment elevation or depression by 1mm in the ECG is a sign of possible alteration in the ionic mechanisms of the channels. Increased amplitude in the ST segment is observed in Brugada syndrome as well as Early Repolarization Syndrom (ERS).[41,42] In both cases along with an elevated ST, the J (Osborn) wave has been identified. The J wave is noted as the deflection that follows the QRS complex. It stems from injury caused in cases of hypothermia and hypercalcemia along with Early Repolarization and Brugada syndromes.[43] The QT interval is the complete activation and recovery of the ventricular myocardium. It is measured from the beginning of the Q wave to the end of the T wave. The length of the QT interval varies with the heart rate (HR). The shortening or lengthening of the HR is dependent on autonomic innervation. To be able to identify disease related changes in the duration of the QT interval, the corrected form is used for analysis (QTc). The QTc is calculated by measuring the length of the QT segment and dividing it by the square root of the duration between two consequtive R waves (R-R interval). A delay in repolarization can result in the Long QT syndrome (LQTS). Twelve different forms of LQTS[44,45] have been idetified based on varying genetic or physiological conditions. LQTS types 1-3 are the most common and are associated with mutations in the subunits of ion channels that are essential in shaping the ventricular AP. Voltage gated ion channels responsible for the depolarizing sodium current, I_{Na}, and the delayed rectifier repolarizing currents, I_{Kr} and I_{Ks}, are the main targets. Lengthening of the QT interval in the ECG occurs in parrallel with increased AP duration in the cardiomyocytes. LQTS can lead to severe arrhythmia and conduction issues. Some of the pathologies observed are syncope, tacharrhythmia, heart failure and sudden cardiac death. In certain cases of LQTS there is also an additional waveform present in the ECG. The U wave is a low amplitude deflection following

the T wave which is mostly observed in V2 and V3 precordial leads.[37] The mechanism behind the U waveform is still being investigated but it has been identified in cases of hypokalemia (low potassium) and its amplitude is enhanced in bradycardia (slow heart rate). In the case of hyperkalemia (elevated extracellular potassium) a peaked T wave is observed in the ECG. Increased potassium raises the overall resting potential of the cardiomyocyte and elevates the slope in phase 3 mediating fast repolarization and shortening of the APD. The decreased APD is connected to an upsurge in conduction through the I_{Kr} channel which is sensitive to extracellular potassium concentration.[46] Upregulation of potassium ion extrusion results in a shortened QT interval and the peaked T wave observed in hyperkalemic patients.[47] The ECG allows for an overview understanding of the electrical activity of the heart during the excitation and relaxation of the myocardium. T wave morphology is the primary focus for uncovering symptoms of deteriorating repolarizing capability of the ventricles. However the length and shape of the waveform does not guarantee a full appreciation of the pathology of the patient, and therefore it must be supplemented by analysis of the dynamic cellular mechanisms.

Ventricular Repolarization and the T wave:

Interpretation of T wave morphology has been controversial, but most recent endeavors have focused on deciphering the role of different cell types in its configuration. Propagation of the electrical signal moves into the ventricles and continues to diffuse from the cells of the apex up to the basal tissue of the heart. Transmurally, the endocardial or the inner most cell layer is activated first. At the end of the QRS most of the myocardium is depolarized ending with the outer epicardial myocytes. The order of repolarization has long been a topic of contention as a multitude of investigations in different species and different experimental preparations present

contradictory results. The pathway of transmural repolarization is considered to be in the reverse direction of depolarization. Three distinct cell layers and tissue regions are identified in the ventricular wall; endocardium, midmyocardium, and epicardium.[53] The outer epicardial cells have the shortest action potential duration (APD). The length of the AP is a product of the dispersed concentration of key ion channels in the cellular membrane. The delayed rectifier potassium current (I_K) leads repolarization in phase 3. The rapid component, I_{Kr}, has on average a homogeneous distribution between epicardial, endocardial and midmyocardial cells. However the slow, I_{Ks} current is more abundant in the outer layer.[59] High concentrations of the repolarizing potassium current has been correlated to the shorter APD observed in epicardial cells. Furthermore the transient outward potassium current (I_{to}) is also an essential contributor to the time of repolarization in the ventricular tissue. $I_{tof,s}$ is responsible for the initial notch identified in phase 1 of the action potential. Epicardial cells have a higher conductance for I_{to} which is visualized in the AP with a more significant notch when compared to the endocardial and midmyocardial cells.[13,14] The inner layer made up of endocardial cells has a prolonged AP when compared to the epicardial tissue. These cells have a decreased concentrations of I_{to} and I_{Ks} ion channels dispersed in their membranes. As a result the conductance for these ionic currents is lower. Existence of midmyocardial cells has been debated, specifically focusing on whether their properties are only visualized experimentally in wedge preparation alone or in coupled cells of the whole heart.[48,53] M cells were first described by experiments of Sicouri and Anzelavitch (1991)[52] performed in a canine ventricular wedge. These cells held unique properties of a significantly longer AP and a depreciated I_{to} notch. Midmyocardial tissue is thought to have a lower distribution and conductance of I_{Ks}. Different animal species have been found to have the

epicardial→endocardial repolarization gradient with varying presence of M cells. Aiba et al., (2005)[56] performed electrophysiological studies on feline ventricular tissue and disected the three transmural layers with the expected proportions of APD being longest in the M cells, followed by the endocardial and then the epicardial cells. Similar findings in other animals such as pig[67], dog,[55] guinea pig[68], and rabbit[57] have been reported with controversy, due to the methodology of single cell patch clamp versus wedge preparation. In a review focusing on the transmural gradient, Wang et al., (2008)[60] concluded that perhaps the discrepancy in the findings is due to animal size. It was hypothesized that M cells have the longest APD in larger animals such as dogs or cows, but are not found in smaller animals such as rabbtis, which and have the longest APD endocardial tissue. However, Taggart et al., (2001)[50] measured unipolar electrograms in 21 intact hearts of human patients and quantified the activation recovery interval (ARI) to analyze the M cell presence. ARI measures the time between the minimum first derivative of the QRS and the maximum derivative of the T wave in an electrocardiogram.[66] ARI is a best approximation of APD in whole heart experiments and therefore can be used in the comparison of cellular properties. They did not find an increased ARI in the midmyocardial region and concluded that the gradient previously described is not viable in the whole heart. Glukhov et al., (2010)[51] analyzed failing and nonfailing human hearts and identified "islands" of M cells with the distinct APD characteristic attributed to the mimyocardial layer. Although the presence of an increased AP duration from the epicardial to the endocardial tissue is emphasized, further research advances can help in fully identifying the incidence and properties of M cells in the human intact heart. In smaller species such as rabbit ventricles, wedge preparations and optical mapping experiments have supported the transmural gradient existence. While studying the

effects of the drug imepadril on action potential heterogeneity in normal and infarcted tissue, Li et al., (2004)[57] measured the APD of the three different regions. Using the current-clamp system, APs were ilicited with an injected depolarizing current and the resultant durations measured. They found that the APD90 (action potential duration at 90% of repolarization) of the midmyocardial myocytes was the longest followed by endocardial cells and then the epicardial tissue. It was also found that the M cells were most susceptible to heart remodelling effects in prolonging the AP. However the limitation of using isolated cells versus intact tissue is present as cell to cell coupling is critical.

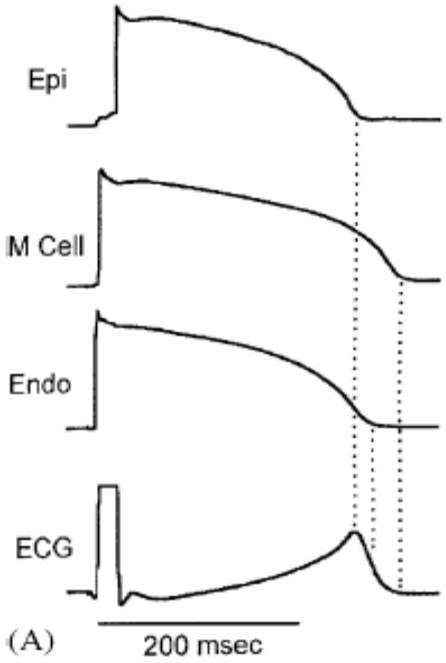

Fig 6: *Transmural APs of the myocardium. Top: Epicardial cell with the shortest APD, denoting T-peak. Middle: M cell with the longest APD, denoting T-end. Bottom: Endocardial cell with intermediate APD identifying the midway region of the downward phase of the T wave. Together the cell layers mediate T wave morphology visualized in the ECG at the bottom. Reproduced from Conrath et al., 2006. Biophysics and Molecular Biology 92, 269-307.*[29]

Idriss et al., (2004)[58] analyzed AP duration at different stages of growth in rabbit ventricular perfused tissue preparations. In transmural regions of the rabbit ventricle, microelectrode APD measurements were collected from the rabbit hearts at 2 weeks, 7 weeks, and at adult ages with varying pacing cycle lengths (PCL). They found as the rabbit aged the midmyocardial region disparity is diminished but the epicardial→endocardial repolarization gradient is maintained. They concluded that the periadolescent rabbit's AP heterogeneity was similar to what was observed in the adult dog wedge prepation. Furthermore at longer pacing cycle lengths there is a greater disperion in APD between subendocardial/midmyocardial cells when compared to the endocardium. The transmural repolarization gradient is considered to have the greatest influence on T wave morphology in the electrocardiogram. T peak (Tp) is the apex of the T wave and is understood to represent the first set of cells repolarizing after activation, which is the epicardial tissue in the ventricular wall. T end (Te) is the return of the T wave to the isoelectric line and the conclusion of repolarization. It is manifested by the tissue with the longest APD, which can either be the midmyocardial or endocardial cells depending on which species is observed.[54,60] However it is not just the transmural gradient that participates in the ECG calculation. The gradient of repolarization between the apex and the base of the heart has an essential function in the shaping the T wave. Direction of the apico-basal gradient varies between animal studies, which have conflicting results in the human, guinee pig, canine, and rabbit heart.[74,64,65] The central point of the debate is whether the direction of repolarization in the vertical axis propagates from apex→base or base→apex. There are significant ramifications that are associated with the pathway of repolarization and therefore a definite understanding must be established. Mantravadi et al., (2007)[62] used optical mapping to identify whole rabbit heart APD.

They found that the repolarization gradient is dependet on the ion channel density of the two components of the I_K current, that are situated in the membrane's of apical and basal cells. Furthermore they determined that the pathway of repolarization travels from the apex to the base of the ventricle in sinus rhythm but is reversed with increased ANS intervention. However their conlcusion does not parallel properties of the electrocardiogram that will only show an upright deflection when the repolarization wave is traveling in the opposite direction of the activation. In this case tissue that was activated first has a shorter APD and therefore repolarization is in the same direction as activation and could not have a direct contribution to the upright T wave observed in the ECG. Taking into account both transmural and apico-basal gradients, Okada et al., (2011)[63] made a 3D model of heart and torso for ECG analaysis. Epicardial, endocardial, and M cells were designated based on AP length and ionic properties. M cell tissue was positioned at either the epicardial or the endocardial side of the ventricular wall in order to investigate the effect of M cell location on the ECG. Furthermore the apico-basal gradient was applied at increasing strength of 0%, 20% and 40% in the model. Respective ECGs were calculated and three pertinent results are identified. First of which is that the M cell should be located towards the endocardial cell layer, otherwise the ECG presented an unphysiological T wave. This is substantiated by in-situ data which associates the longest APD in most species with the subendocardial region. The second finding is that not having a transmural gradient in the ventricle results in an inverted T wave in most leads. They also concluded that a really strong apico-basal gradient is necessary to demonstrate an upward deflection in the ECG. However the gradient that is applied in their model has the activation and repolarization traveling in the same direction. The apex→base repolarization gradient would not be expected to manifest an upright

T wave. Therefore their investigation does not clearly decipher the relationship between the apico-basal gradient and T wave morphology. In a more recent publication, Janse et. al(2012)[72] analyzed previous experiments and highlighted discrepancies in the current understanding of the roles of both the transmural and apico-basal gradients. They concluded that the transmural gradient is minimal, but primarily in dog wedge preparations. They believe that the human T wave is a product of the apico-basal gradient only with base→apex repolarization. Therefore the morphology observed in the ECG comes from the basal cardiomyocytes repolarizing before the apical cells, giving an inverse relationship between activation and repolarization. This analysis is substantiated with the previous work of Cowan et. al (1988)[73], in which fifteen patients undergoing either routine coronary artery bypass grafting or aortic valve replacement were analyzed. Monophasic action potentials were recorded intraoperatively in each patient. They gathered APD data four times from ten sites on the left ventricle. It was found that repolarization time has an inverse relationship with activation time, presenting the base→apex repolarization gradient. Furthermore Cheng et. al (1999)[71] performed whole cell clamp experiments to identify regional differences in the potassium current (I_K) which dictates repolarization. The investigation determined that APD in the apex is longer than the APD of the base, insinuating the base→apex repolarization gradient. However the measurements were achieved at a PCL of 1Hz which is longer than the rabbit's fast heart rate. A longer pacing cycle length can affect recovery of the ionic channels and can influence the resulting AP duration. Single cell experimental techniques are also less preferable as a tool for extrapolation to whole tissue, due to the importance of cell-cell coupling. Intact human heart ARIs were measured by Ramanthan et. al (2006)[61] using noninvasive electrocardiographic imaging (ECGI). Seven patients participated in order to gather

information on activation and repolarization of the ventricle on the epicardial surface. The activation sequence was as expected from the apical to basolateral tissue and in their findings, repolarization followed in the same direction. This finding further adds to the complexity of the apico-basal gradient. Therefore in order to elucidate the mechanism of the upright T wave the transmural gradient will be incorporated with the apex→base and the base→apex gradients in this experiment. Understanding repolarization is necessary for treating arrhythmia. Cardiovascular diseases can cause differences in repolarization time (RT) in the myocardium and thus affect the T wave. Repolarization time is the duration from depolarization of the cardiomyocyte to the full recovery of excitability. It is calculated by summing the AP duration with the activation time (AT) as the varying regions of the ventricle depolarize at different moments. Dispersion of repolarization (DOR) is used to asses tissue vulnerability to conduction block and reentry. DOR is the difference between the shortest and the longest repolarization time in a set of measurements.[60] Dispersion can be analzyed globally in which the RT quantities are gathered from different regions without consideration of the spatial distribution. Global dispersion allows for an overview of activity, but limits understanding of the regions that the RTs originate from. Local dispersion measurement of longest and shortest repolarization time is therefore used to asses location specific differences. For example regions with similar average global dispersion may vary when the local RTs are isolated. A significant difference in repolarization can increase susceptability for arrhythmia. Furthermore the size of the region and slow conduction velocity can increase the occurrence of reentry. Thus when cellular recovery from depolarization varies greatly a propagating wave can be blocked causing surrounding regions with shorter refractory periods to be reactivated. Maximal dispersion between adjacent

sites in the myocardium can be proarrhythmic and therefore a target for treatment and prevention. Pathological and drug induced condition that affect the repolarization gradients can cause T wave changes in width and height. An in-silico model of the ventricle will be used to manifest the T wave and deduce the accurate direction of repolarization.

Materials & Methods:

I. Rabbit Data:

In-situ data gathered from rabbit cardiomyocytes and intact rabbit tissue is applied in making a virtual model of the rabbit ventricle with nine distint cell types. Transmural activation and repolarization of the rabbit ventricle is attained from Idriss et. al (2004)[58]. The action potential durations attained at PCL of 500 ms is used. The rabbits' average age was around 7 weeks where a more distinct prolonged APD is observed in the subendocardium. Extracting subendocardial values parallels the rabbit model to the human heart data which points to the presence of M cells in the myocardium. The epicardial (APD_{90}=149ms), endocardial (APD_{90}=166ms) and subendocardial (APD_{90}=170ms) values were taken to represent the transmural gradient of the rabbit. For apical and basal cell APD Mantravadi et. al (2007)[62] was analyzed. In their work on intact rabbit tissue they found the apical APD_{90} = 159ms and the basal APD_{90} = 176ms. When applying the reverse gradient of repolarization from base→apex, the opposite difference in AP length is assumed. In both transmural and apico-basal directions the average the dispersion in APD resulted in the shortest values being 90% of the longest APD. Therefore to reproduce the in-situ differences in the ucla model cell layers, a similar proportion is maintained.

II. Simulation Model

The UCLA rabbit ventricular action potential cell model is used as the basis for creating the nine cell types that was incorporated in the virtual ventricle. The Mahajan et. al (2008)[76] model comprehensively represents ion channels, their kinetics, and their dynamic interactions. In order to create a cell from the epicardial (Epi), endocardical (Endo), midmyocardial (M), apical, or basal region changes are made to the conduction of the participating ionic currents. (Table 1) To test whether the original cell in the Mahajan model is from the epicardium, midmyocardium, or endocardium, the model was run in a 1D cable at a short (400ms) and a long (1s) pacing cycle length. According to Fedida et. al (1991)[77] investigation, the rabbit only has a prominent notch observed in the epicardial cell at long pacing cycle lengths (PCL). When the Mahajan cell model was paced at 400ms. no notch was present but at a longer PCL the epicardial notch was visible. (Fig. 7) Thus the current ucla model cell is a rabbit epicardial cell and whether it should be located in the apex or base of the ventricle would be decided via further simulation. Further changes are made to the model to create the physiological APD differences observed in the ventricle. The shape and duration of repolarization in the action potential stems from the current density of the slow component of the delayed rectifier potassium current and the fast component of the rapid inward potassium current. Modifications to the conduction of I_{Ks} and $I_{to,f}$ is used to create the 9 cells with distinct APDs. Changes were made to $G_{to,f}$=.055mS/µF and G_{Ks}=.32 mS/µF in the 1D cable that resulted in the transmural and apico-basal gradients. The formulation of the 9 cell types took into account if the Epi, Endo or M cell is found in the base, center, or apex of the ventricle. The goal was to reproduce the gradients that have been experimentally identified[58,62], giving a proportion of 90% difference of the shortest APD from

the longest APD in each direction. A transmural gradient was formed, with the APD epicardium < APD endocardium < APD M Cell. In order to deduce the apico-basal direction of repolarization, two versions of the gradient are simulated. An apex→base repolarization gradient where APD apex < APD base and a reverse base→apex gradient where APD base < APD apex are applied. The resulting 1D cable APD values are presented in Table 1 (A & B) along with corresponding changed to the conduction of the respective ion currents.

A.

Repolarization: Epi to Endo & Apex to Base	$G_{to,f}$ (mS/µF)	G_{Ks} (mS/µF)	APD (ms)
Base Endo	0.055	0.256	211
Base M	0.055	0.218	219
Base Epi	0.110	0.320	187
Center Endo	0.055	0.320	200
Center M	0.055	0.288	205
Center Epi	0.110	0.480	173
Apex Endo	0.055	0.432	186
Apex M	0.055	0.384	192
Apex Epi	0.110	0.640	164

B.

Repolarization: Epi to Endo & Base to Apex	$G_{to,f}$ (mS/µF)	G_{Ks} (mS/µF)	APD (ms)
Base Endo	0.055	0.432	186
Base M	0.055	0.384	192
Base Epi	0.110	0.640	164
Center Endo	0.055	0.320	200
Center M	0.055	0.288	205
Center Epi	0.110	0.480	173
Apex Endo	0.055	0.256	211
Apex M	0.055	0.218	219
Apex Epi	0.110	0.320	187

Table 1: *Values of the 9 Distinct Cell Types:* **(A)** *Epi→endo and apex→base repolarization gradients.* **(B)** *Epi→endo and apex→base repolarization gradients. Respective APDs resulted from changed to conductance of the two main currents ($G_{to,f}$ & G_{Ks}).*

The resulting state variables for each of the cell types are incorporated into a 3D model of the ventricle with purkinje activation. Using the virtual electrocardiogram (Eq.1) described in Xie et. al (2004)[75] six different scenarios were tested in-silico.

$$ECG = \iiint \sum_{i=1}^{3} \sum_{j=1}^{3} \tilde{D}_{i,j} (\nabla V)_j (\nabla (1/R))_i dxdydz$$

Eq 1: *Calculation of the virtual electrocardiogram. Where V is voltage, D is the diffusion tensor, and R is the distance from a lead to the location of the dipole. Reproduced from Xie et al., 2004. Journal of Clinical Investigation 113 (5) 686-693.* [75]

III. Experimental Set Up

I. Homogeneous	Endo	M	Epi	II. Trans & No Apex/Base	Endo	M	Epi
Base	187	187	187	Base	211	219	187
Center	187	187	187	Center	211	219	187
Apex	187	187	187	Apex	211	219	187
III. No Trans & Apex<Base	Endo	M	Epi	IV. No Trans & Base<Apex	Endo	M	Epi
Base	187	187	187	Base	164	164	164
Center	173	173	173	Center	173	173	173
Apex	164	164	164	Apex	187	187	187
V. Trans & Apex<Base	Endo	M	Epi	VI. Trans & Base<Apex	Endo	M	Epi
Base	211	219	187	Base	186	192	164
Center	200	205	173	Center	200	205	173
Apex	186	192	164	Apex	211	219	187

Table 2. *Six simulations (I-VI) are made in the 3D ventricle for calculation of an in-silico ECG. Respective APDs for each experiment are given for the 9 cell regions. Homogeneous **(I)**, transmural alone **(II)**, apex→base **(III)**, base→apex **(IV)**, and combined transmural with two different apico-basal gradient are analyzed **(V & VI)**.*

Two main iquiries were focused on in setting up the six simulations of the rabbit ECG. First, the contribution of either the transmural or the apico-basal repolarization gradient in T wave morphology. Second, to find the accurate direction of the apico-basal gradient that results in the appropriate physiological T wave. Six different ventricular myocardium were simulated and their corresponding ECGs calculated. (Table 2) The first was a homogeneous ventricle (Table 2, I) with no transmural or apico-basal gradients, where APD Epi, Endo, M, apex, and base were all equivalent. Then a transmural repolarization gradient is applied, having APD Epi < APD Endo < APD M (Table 2, II). To see the effect of apico-basal gradient alone, two simulations are used, one with APD apex < APD base (Table 2, III) and another with the reverse gradient of APD base < APD apex (Table 2, IV). In the last two simulations a combination of the transmural and apico-basal repolarization gradient is simulated. The epi→endo gradient is applied simultaneously with

both an apex → base gradient (Table 2, V) and with the base → apex repolarization gradient (Table 2, VI) as well. To assess the validity of each resulting ECG a comparison to an in-situ rabbit electrocardiogram is utilized.[78] (Fig. 9)

Results:

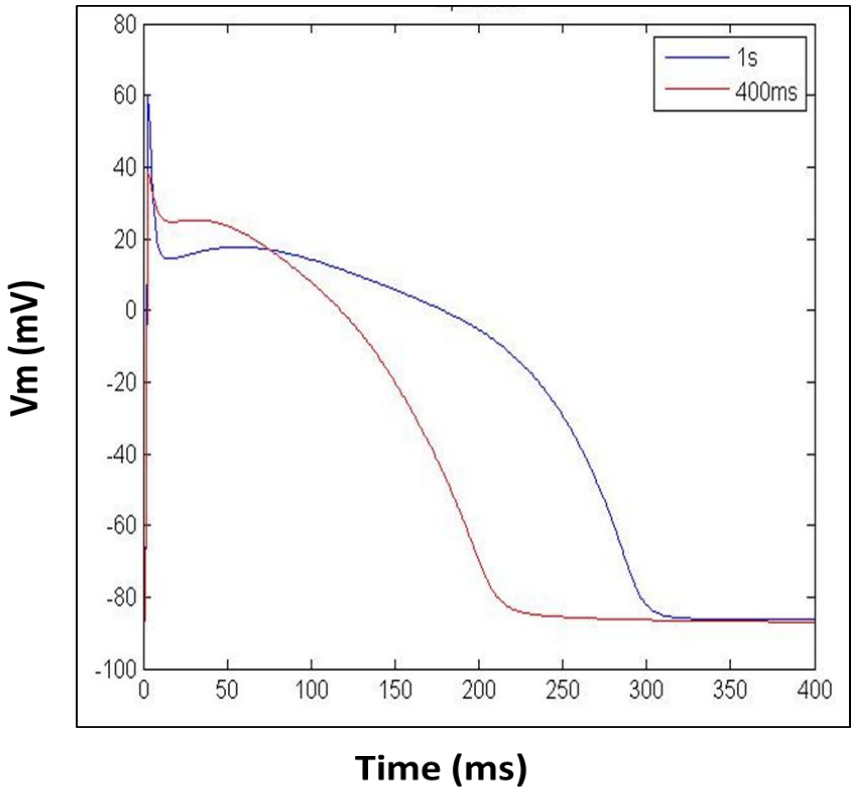

Figure 7. *Action potentials of the Mahajan rabbit cell model paced at a fast 400ms (Red Trace) and slow 1s (Blue Trace) pacing cycle length. The AP presents a strong initial repolarization notch at the long cycle length. Thus the cell model is originates in the epicardium of the ventricular wall. .*

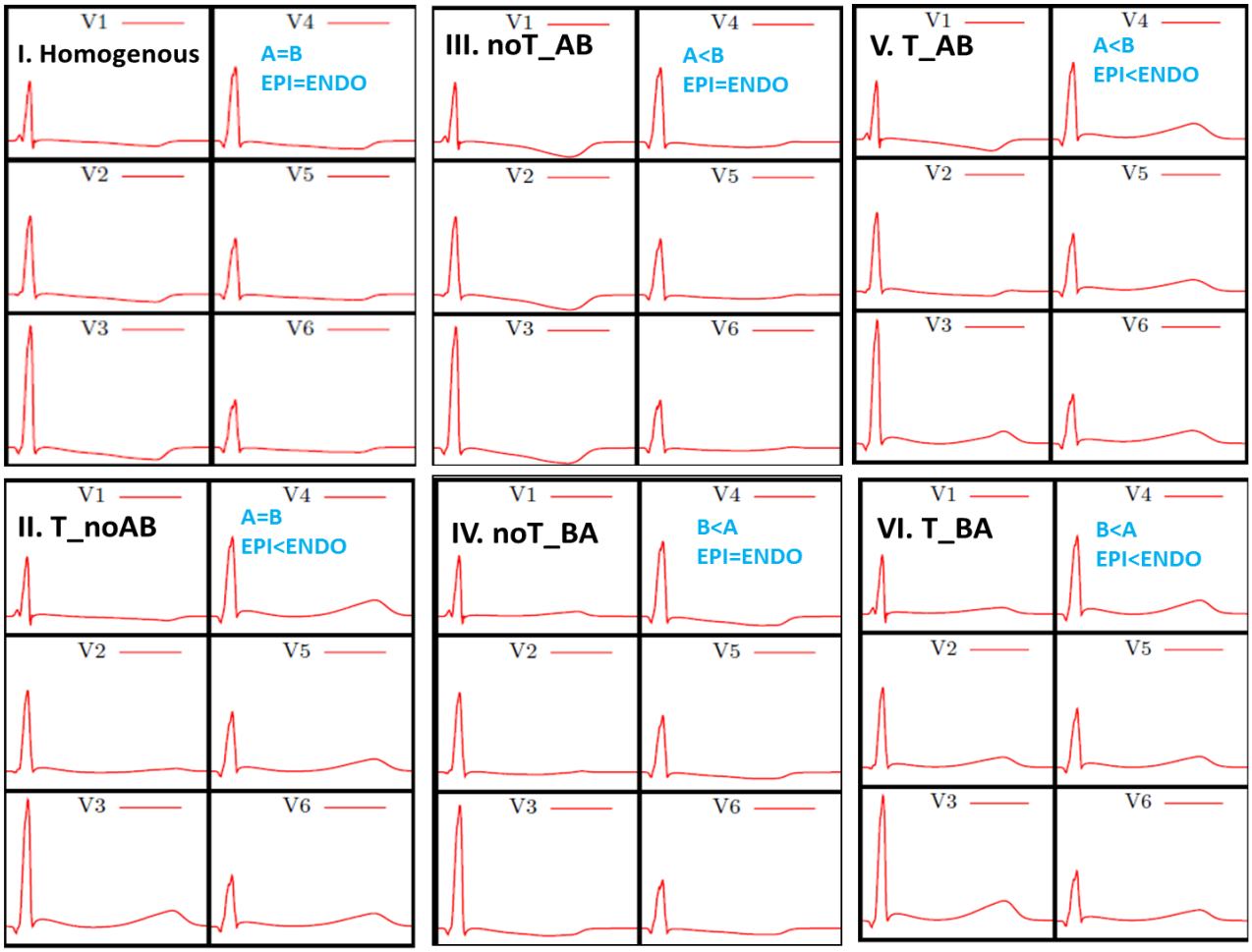

Fig 8: *ECG results of 6 simulation experiments. In simulation **I-VI** the QRS complex and the T wave are visualized in each of the 6 Precordial Leads (V1-V6). In each ECG, the V1 box contains a description of the gradients present and in the V2 box the differences in APD of both the transmural and apico-basal gradients are given. T= transmural gradient, A=APD apex, B = APD base, Epi = APD epicardium, Endo = APD endocardium.*

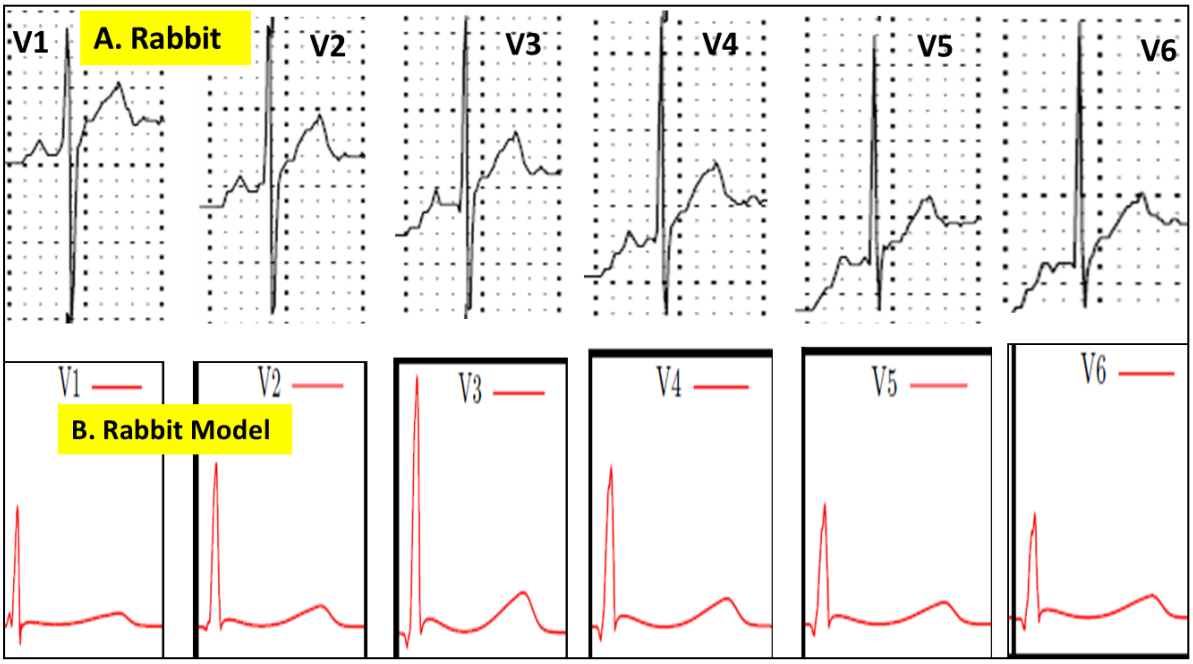

Figure 9: (A) *Recorded rabbit ECG*[78] *given with precordial leads V1-V6, showing the QRS complex and the T wave.* **(B)** *The resulting best ECG simulation that gives a physiologically accurate upright T wave in V1-V6. Transmurally, APD epi is shorter than APD endo, and apicobasally, APD base is shorter than APD apex.*

Discussion:

Cell modeling combinded with a virtual ECG is a powerful tool for analysis and understanding of physiological processes in the heart. The incorporation of the 9 cell types into the 3D ventricle illuminated the significance of repolarizing currents in T wave morphology. The six simulations presented interesting findings. The ECG for the homogeneous ventricle (Fig. 8,I), with APD = 187ms in all directions resulted in an inverted T wave in all six precordial leads. Applying the transmural gradient which created a distinction in epi, endo, and M cell layers through apex, center and base (Fig. 8, II) began to show a more physiological representation of the ECG. Although V1 and V2 were still inverted leading to the conclusion that the transmural gradient is not alone in defining the T wave. The simulations without the transmural gradient and with

variation in apico-basal gradient did not create an accurate ECG. However the apex → base gradient's ECG had a more pronounced inverted T wave in V1-VIII precordial leads (Fig. 8, III). Combining the transmural gradient with the two apico-basal gradients illuminated in simulation the properties of the physiological T wave. The apex→base repolarization gradient along with the transmural gradient (epi→endo) resulted in an upright T wave in V3-V6 precordial leads, but had an unphysiological T wave in V1 and V2 (Fig. 8, V). The sixth simulation, containing both the transmural (epi→endo) and a base→apex repolarization gradient resulting ECG had an upright T wave in all six precordial leads (Fig. 8, VI). The most accurate sixth simulation best represents what was observed in-situ in the rabbit ECG (Fig. 9). In both the simulated and experimental electrocardiogram an upright T wave is visualized throughout the six precordial leads. A conclusion can be made that indeed the transmural and apico-basal gradients partake in the formation of the T wave. APD epi must be shorter than APD endo and apico-basal APD base must be shorter than APD apex. The APD dispersion between the different regions of the ventricle is due to the channel density and therefore conduction of the I_{Ks} and $I_{to,f}$ repolarizing currents. Connecting the cellular dynamics to the results observed on the surface ECG is essential in understanding the pathological mechanisms behind observed arrhythmias. T wave changes can now be attributed to deviations in repolarization properties and therefore modification to the key ion channels can present a benefit. Previous discrepancies in experimental results with different directional understanding of the apico-basal repolarization gradient can be associated with the impediment of using certain techniques such as individual patch clamp method which removes the cell-cell coupling necessary to view the diffusion in the myocardium. Also injection of activating current into a certain region of a wedge preparation

does not directly parallel the conduction system of the heart and can have varied results. Thus simulation presents the opportunity to understand repolarization in whole heart tissue with purkinje activation. The information gathered from the rabbit cell model can be applied to the human heart. Panfilov et. al (2006)[69] found much similarity between the two species when studying ventricular fibrillation in both animals. The 3D virtual ventricle with the 9 designated cells can be used to study T wave specific pathologies such as hyperkalemia, LQTS, and ST segment deviations. Future investigations into lead placement, ion channel kinetics, and pharmacological intervention can provide further understanding of what is occurring at both the cellular and whole tissue level via in-silico methods.

References:

1. Wang Y, Hill JA. Electrophysiological Remodelin in Heart Failure. J Mol Cell Cardiol. 2010; 48(4): 619-632.
2. Baruscotti M, DiFrancesco D, Accili EA. From Funny Current to HCN Channels: 20 Years of Excitation. News Physiol. Sci. 2002; 17: 33-37.
3. Boyett MR, Honjo H, Kodama I. The sionatrial node, a heterogeneous pacemaker structure. Cardiovascular Research. 2000; 47: 658-687.
4. Meek S, Morris F. ABC of clinical electrocardiography. BMJ. 2002; 524: 415-418.
5. Dhein S. Pharmacology of gap junctions in the cardiovascular system. Cardiovascular Research. 2004; 62: 287-298.
6. Mazgalev TN, Ho SY, Anderson RH. Anatomic-Electrophysiological Correlations Concerning the Pathways for Atrioventricular Conduction. Circulation. 2001; 103: 2660-2667
7. Rohr S. Role of gap junctions in the propagation of the cardiac action potential. Cardiovascular Research. 2004; 62: 309-322.
8. Sarma JD, Meyer RA, Wang FW, Abraham V, Lo CW, Koval M. Multimeric connexin interactions prior to the tran-Golgi network. Journal of Cell Science. 2001; 114: 4013-4024.
9. Cottrell TG, Burt JM. Heterotypic gap junction channle formation between heteromeric and homomeric Cx40 and Cx43 connexons. Am J Physiol. 2001; 281: C1559-C1567.
10. Spray DC, Suadicani SO, Srinivas M, Gustein DE, Fishman GI. Gap Junctions in the cardiovascular system. Comprehensive Physiology. 2011; 169-211.
11. Ravens U, Cerbai E. Role of potassium currents in cardiac arrhythmias. Europace. 2008; 1-5.
12. Luo CH, Ruby Y. A dyanmic model of the cardiac ventricular action potential . I. Simulation of ionic currents and concentration changes. Circulation Research. 1994; 74: 1071-1096.
13. Bassani RA. Transient outward potassium current and Ca^{2+} homeostasis in the heart: beyond the action potential. Brazilian Journal of Medical and Biological Research. 2006; 39: 393-403.
14. Patel SP, Campbell DL. Transient outward potassium current, 'I_{to}', phenotypes in the mammmalian left ventricle: underlying molecular, cellular and byiophysical mechanisms. J Physiol. 2005; 569.1: 7-39.
15. Bers DM. Cardiac excitation-contraction coupling. Nature. 2002; 415: 198-205.
16. Periasamy M, Huke S. SERCA Pump Level is a Critical Dterminant of Ca^{2+} Homeostasis and Cardiac Contractility. J Mol Cell Cardio. 2001; 33: 1053-1063.
17. Nichols CG, Lopatin AN. Inward Rectifier Potassium Channels. Annu. Rev. Physiol. 1997; 59: 171-91.
18. Li GR, Dong MQ. Revisit of the Cardiac Inward Rectifier Potassium Current I_{K1}. The Open Circulation and Vascular Journal. 2010; 3: 95-102.
19. Farid TA, Nair K, Masse S, Azam MA, Maguy A, Lai PFH, Umapathy K, Dorian P, Chauhan V, Varro A, Al-Hesayen A, Waxman M, Nattel S, Nanthakumar K. Role of K_{ATP} Channels in the Maintenance of Ventricular Fibrillation in Cardiomyopathic Human Hearts. Circulation Research. 2011; 109: 1309-1318.
20. Grover GJ, Garlid KD. ATP-Sensitive Potassium Channels: A Review of their Cardioprotective Pharmacology. J Mol Cell Cardiol. 2000; 32: 677-695.

21. Nerbonne JM, Kass RS. Molecural Physiology of Cardiac Repolarization. Physiol Rev. 2005; 85: 1205-1253.
22. Triposkiadis F, Karaynnis G, Giamouzis G, Skoularigis J, Louridas G, Butler J. They Sympathetic Nervous System in Heart Failure. Physiology, Pathophysiology, and Clinical Implications. Journal of the American College of Cardiology. 2009; 54 (19): 1747-1762.
23. Zipes DP. Heart-brain interactions in the cardiac arrhythmias: Role of the autonomic nervous system. Cleveland Clinic Journal of Medicine. 2008; 75: 894-896.
24. Kaumann A, Bartel S, Molenaar P, Sanders L, Burrell K, Vetter D, Hempel P, Karczewski P, Krause EG. Activation of β_2-Adrenergic Receptors Hastens Relaxation and Mediates Phosphorylation of Phospholamban, Troponin I, and C-Protein in Ventricular Myocardium From Patients With Terminal Heart Failure. Circulation. 1999; 99: 65-72.
25. Ahmed A. Myocardial beta-1 adrenoceptor down-regulation in aging and heart failure: implications for beta-blocker use in older adults with heart failure. The European Journal of Heart Failure. 2003; 5: 709-715.
26. Brodde OE, Michel MC. Adrenergic and Muscarinic Receptors in the Human Heart. Pharmacological Reviews. 1999; 51(4): 651-689.
27. Knowlton KU, Michel MC, Itani M, Shubeita HE, Ishihara K, Brown JH, Chien KR. The α_{1A}-Adrenergic Receptor Subtype Mediates Biochemical Molecular, and Morphologic Features of Cultured Myocardial Cell Hypertrophy. The Journal of Biological Chemistry. 1993; 268(21): 15374-15380.
28. Olshansky B, Sabbah HN, Hauptman PJ, Colucci WS. Parasympathetic Nervous System and Heart Failure: Pathophysiology and Potential Implications for Therapy. Circulation. 2008; 118: 863-871.
29. Malvivuo J, Plonsey R. Principles and Applications of Bioelectric and Biomagnetic Fields. Oxford University Press. 1995; 121-124.
30. Kishi T. Heart failure as an autonomic nervous system dysfunction. Journal of Cardiology. 2012; 59: 117-122.
31. Dupre A, Vincent S, Iaizzo, PA. Basic ECG Theory, Recordings, and Interpretation. Handbook of Cardiac Anatomy, Physiology, and Devices. 2005; 191-201.
32. Durrer D, Van Dam R. TH, Freud GE, Janse MJ, Meijler FL, Arzbaecher RC. Total Excitation of the Isolated Human Heart. Circulation. 1970; 41: 899-912.
33. Einthoven, W. The Human Electrocardiogram. The Lancet. 1912; 853-861.
34. Wilson FN, Johnston FD, Macleod AG, Baker PS. Electrocardiograms that represent the potential variations of a single electrode. The American Heart Journal. 1934 ; 447-458.
35. Okamoto Y, Mashima S. The zero potential and Wilson't central terminal in electrocardiography. Bioelectrochemistry and Bioenergetics. 1998; 47: 291-295.
36. Yan GX, Lankipalli RS, Burke JF, Musco S, Kowey PR. Ventricular repolarization components on the electrocardiogram: Cellular basis and clinical significance. J. Am. Coll. Cardiol. 2003; 42: 401-409.
37. Rautaharju PM, Surawicz B, Gettes LS. AHA/ACCF/HRS Recommendations for the Standardization and Interpretation of the Electrocardiogram: Part IV: The ST Segment, T and U Waves, and the QT Interval a Scientific Statement From the American Heart Association

Electrocardiography and Arrhythmias Committee, Council on Heart Rhythm Society Endorsed by the International Society for Computerized Electrocardiology. J. Am. Coll. Cardiol. 2009; 53: 982-991.
38. Kashani A, Barold S. Significance of QRS Complex Duration in Patients With Heart Failure. Journal of the American College of Cardiology. 2006; 46 (12): 2183-2192.
39. Chatterjee S, Changawala N. Fragmented QRS Complex: A Novel Marker of Cardiovascular Disease. Clinical Cardiology. 2009; 33 (2): 68-71.
40. Das MK, Khan B, Jacob S, Kuma A, Mahenthiran J. Significance of a Fragmented QRS Complex Versus a Q Wave in Patients With Coronary Artery Disease. Circulation. 2006; 113: 2495-2501.
41. Yan GX, Antzelevitch C. Cellular Basis for the Brugada Syndrome and Other Mechanisms of Arrhythmogenesis Associated With ST-Segment Elevation. Circulation. 1999; 100: 1660-1666.
42. Gussak I, Antzelevitch C. Early Repolarization Syndrome: Clinical Characteristics and Possible Cellular and Ionic Mechanisms. Journal of Electrocardiology. 2000; 33 (4): 299-309.
43. Antzelevitch C, Yan GX. J wave syndromes. Heart Rhythm. 2010; 7 (4): 549-558.
44. Roden DM. Long-QT Syndrome. New England Journal of Medicine. 2008; 358 (2): 169-176.
45. Bokil NJ, Baisden JM, Radford DJ, Summers KM. Molecular genetics of long QT syndrome. Molecular Genetics and Metabolism. 2010; 101: 1-8.
46. Dittrich KL, Walls RM. Hyperkalemia: ECG Manifestations and Clinical Consideration. The Journal of Emergency Medicine. 1986; 4: 449-455.
47. Parham WA, Mehdirad AA, Biermann KM, Fredman CS. Hyperkalemia Revisited. Tex Heart Inst J. 2006; 33: 40-47.
48. Conrath CE, Wilders R, Coronel R, Bakker JMT, Taggart P, Groot JR, Opthof T. The relevance of M cells in the human heart and their role in the endo-epicardial gradient of repolarization. Presented at Einthoven Symposium in Leiden, The Netherlands (2002) and at the 26th Scientific Sessions of the Heart Rhythm Society. New Orleans (2005). Chapter 3: 1-29.
49. Conrath CE, Opthof T. Ventricular repolarization: An overview of (patho)physiology, sympathetic effects and genetic aspects. Biophysics and Molecular Biology. 2006; 92: 269-307.
50. Taggart P, Sutton PMI, Opthof T, Coronel R, Trimlett R, Pugsley W, Kallis P. Transmural repolarisation in the left ventricle in humans during normoxia and ischaemia. Cardiovascular Research. 2001; 50: 454-462.
51. Glukhov AV, Fedorov VV, Lou Qing, Rvikumar VK, Kalish PW, Schuessler RB, Moazami N, Efimov IR. Transmural Dispersion of Repolarization in Failing and Nonfailing Human Ventricle. Circulation Research. 2010; 106: 981-991.
52. Sicouri S, Antzelevitch C. A subpopulation of cells with unique electrophysiological properties in the deep subepicardium of the canine ventricle. The M cell. Circulation Research. 1991; 68: 1729-1741.
53. Patel C, Burke JF, Patel H, Gupta P, Kowey PR, Antzelevitch C, Yan GX. Is there a significant transmural gradient in repolarization time in the intact heart? Cellular Basis of the T Wave: A Centuty of Controversy. Circ Arrhythm Electrophysiol 2009; 2:80-88.
54. Antzelevitch C. Transmural dispersion of repolarization and the T wave. Cardiovascular Reasearch. 2001; 50: 426-431.

55. Balati B, Varro A, Papp JG. Comparison of the cellular electrophysiological characteristics of canine left ventricular epicardium, M cells, endocardium and Purkinje fibres. Acta Physiol Scand. 1998; 164: 181-190.
56. Aiba T, Shimizu W, Inagaki M, Noda T, Miyoshi S, Ding WG, Zankov DP, Toyoda F, Matsuura H, Minoru H, Sunagwa K. Cellular and Ionic Mechanism for Drug-Induced Long QT Syndrome and Effectiveness of Verapamil.
57. Li Y, Xue Q, Ma J, Zhang C, Qiu P, Wang L, Gao W, Cheng R, Lu Z, Wang S. Effects of imidapril on heterogeneity of action potential and calcium current of ventricular myocytes in infaracted rabbits. Acta Pharmacol Sin. 2004; 25 (11): 1458-1463.
58. Idriss SF, Wolf PD. Transmural Action Potential Repolarization Heterogeneity Develops Postnatally in the Rabbit. Journal of Cardiovascular Electrophysiology. 2004; 15 (7): 795-801.
59. Xu X, Rials SJ, Wu Y, Salata JJ, Liu T, Bharucha DB, Marinchak RA, Kowey PR. Left Ventricular Hypertrophy Decreases Slowly but Not Rapidly Activating Delayed Rectifier Potassium Currents of Epicardial and Endocardial Myocytes in Rabbits. Circulation. 2001; 103: 1585-1590.
60. Wang D, Patel C, Cui C, Yan GX. Precelinical assesment of drug-induced proarrhythmias: Role of arterially perfused rabbit left ventricular wedge preparation. Pharmacology & Therapeutics. 2008; 119: 141-151.
61. Ramanthan C, Jla P, Ghanem R, Ryu K, Rudy Y. Activation and repolarization of the normal human heart under complete physiological conditions. PNAS. 2006; 16: 6300-6314.
62. Mantravadi R, Gabris B, Liu T, Choi BR, Groat WC, Ng GA, Salama G. Autonomic Nerve Stimulation Reverses Ventricular Repolarization Sequence in Rabbit Hearts. Circulation Research. 2007; 100: 72-80.
63. Okada J, Washio T, Maehara A, Momomura S, Sugiura S, Hisada T. Transmural and apicobasal gradients in repolarization contribute to T-wave genesis in human surface ECG. Am J Physiol Heart Circ Physiol. 2011; 301: H200-H208.
64. Nagase S, Kusano KF, Morita H, Nishii N, Sakuragi S, Ohe T. Longer Repolarization in the Epicardium at the Right Ventricular Outlow Tract Causes Type 1 Electrocardiogram in Patients With Brugada Syndrome. J. Am. Coll. Cardiol. 2008; 51: 1154-1161.
65. Szentadrassy N, Banyasz T, Biro T, Szabo g, Toth BI, Magyar J, Lazar J, Varro A, Kovacs L, Nanasi PP. Apico-basal inhomogeneity in distribution of ion channels in canine and human ventricular myocardium. Cardiovascualr Research. 2005; 65: 851-860.
66. Burton FL, Cobbe SM. Dispersion of ventricular repolarization and refractory period. Cardiovascular Research. 2001; 50: 10-23.
67. Stankovicova T, Szilard M, Scheerder I, Sipido K. M cells and transmural heterogeneity of action potential configuration in myocytes from the left ventricular wall of the pig heart. Cardiovasc. Res. 2000; 45: 952–960.
68. Sicouri S, Quist M, Antzelevitch C. Evidence for the presence of m cells in the guinea pig ventricle. J. Cardiovasc. Electr. 1996; 7: 503–511.
69. Panfilov AV. Is heart size a factor in ventricular fibrillaiton? Or how close are rabbit and human hearts? Heart Rhythm. 2006; 3 (7): 862-864.

70. Bernardo D, Murray A. Explaiing the T-wave shape in the ECG. Nature. 2000; 403 (6): 43.
71. Cheng J, Kamiya K, Liu W, Tsuji Y, Toyama J, Kodama I. Heterogeneous distribution of the two components of delayed rectifier K+ current: a potential mechanism of the proarrhythmic effects of methanesulfonanilideclass III agents. Cardiovascular Research. 1999; 43: 135-147.
72. Janse MJ, Coronel R, Opthof T, Sosunov EA, Anyukhovsky EP, Rosen MR. Repolarization gradients in the intact heart: Transmural or apico-basal? Progress in Biophysics and Molecular Biology. 2012 1-10.
73. Cowan JC, Hilton CJ, Griffiths CJ, Tansuphaswadikul S, Bourke JP, Murray A, Campbell RWF. Sequence of epicardial repolarisation and configuration of the T wave. Br Heart J. 1988; 60: 424-433.
74. Keller DUJ, Weiss DL, Dossel O, Seemann G. Influence of I_{Ks} Heterogeneithies on the Genesis of the Twave: A Computational Evaluation. IEEE Transactions on Biomedical Engineering. 2012; 59: 311-322.
75. Xie F, Qu Z, Yang J, Baher A, Weiss JN, Garfinkel A. A simulation study of the effects of cardiac anatomy in ventricular fibrillation. The Journal of Clinical Investigation. 2004; 113 (5): 686-693.
76. Mahajan A, Shiferaw Y, Sato D, Baher A, Olcese R, Xie LH, Yang MJ, Chen PS, Restrep JG, Karma A, Garfinkel A, Qu Z, Weiss JN. A Rabbit Ventricular Action Potential Model Replicating Cardiac Dynamics at Rapid Heart Rates. Biophysical Journal. 2008; 94: 392-410.
77. Fedida D, Giles WR. Regional Variations in Action Potentials and Transient Outward Currrent in Myocytes Isolated From Rabbit Left Ventricle. Journal of Physiology. 1991; 442: 191-209.
78. Dr. Olujimi Ajijola, Personal Communication. 2012